

# Documentation for MEMLS, Version 3

## Microwave Emission Model of Layered Snowpacks

Christian Mätzler and Andreas Wiesmann  
April 2007, revised May 2012, July 2014  
Institute of Applied Physics - University of Bern  
Sidlerstrasse 5, 3012 Bern, Switzerland  
Phone ++ 41 31 631 89 11 - Fax ++ 41 31 631 37 65  
matzler@iap.unibe.ch

### 1. Abstract

A thermal Microwave Emission Model of Layered Snowpacks (MEMLS) was developed for the frequency range, 5 to 100 GHz (Mätzler, 1996b; Wiesmann and Mätzler, 1999; Mätzler and Wiesmann, 1999). It is based on radiative transfer, using six-flux theory to describe multiple volume scattering and absorption, including radiation trapping due to internal reflection and a combination of coherent and incoherent superposition of reflections between layer interfaces. The scattering coefficient was determined empirically from measured snow samples (Wiesmann et al. 1998), whereas the absorption coefficient, the effective permittivity, refraction and reflection at layer interfaces were based on physical models and on measured ice dielectric properties. The number of layers is only limited by computer time and memory. A limitation of the empirical fits and thus of MEMLS is in the range of observed frequencies and correlation lengths (a measure of grain size). First model validation for dry winter snow was successful.

MEMLS has been coded in MATLAB. It forms part of a combined land-surface-atmosphere microwave radiation model for radiometry from satellites [Pulliainen *et al.*, 1998].

**Version 3**, described here, uses updated formulas for the dielectric constants of ice and water, including slightly saline ice, to account for salt-contaminated snow on sea ice (Chapter 5.3 in Mätzler et al. 2006). For pure ice the update is a very small change in the imaginary part of the dielectric constant, since the formulas used in Versions 1 and 2 were mainly confirmed with new measurements. However, the salinity also affects the imaginary part even at the level of a few ppm; the increase is significant if the temperature approaches the melting point of ice. The applicable salinity range covers 0 to 0.1 ppt, but may still work up to 1 ppt.

The dielectric constant of water is used in case of wet snow. Here we use the two-Debye relaxation formula of Liebe et al. (1991). Although more accurate formulations exist (Ellison, Chapter 5.2, in Mätzler et al. 2006; Ellison, 2007), the simplicity of Liebe's expression is an advantage, and the accuracy is sufficient in view of the limited knowledge on the liquid-water content in wet snow.

In addition the distinction on scattering between different types of snow can now be specified by a *graintype* parameter with *graintype*=1 for natural dry snow as observed by Mätzler (1996a), *graintype*=2 for spherical scatterers, and *graintype*=3 for thin spherical shells (see routine descriptions). The current option is *graintype*=1.

In May 2012 the text was improved, especially near Equations (57a,b) to better describe the behavior of the effective incidence angle. In 2014 the function *fresnelc.m* was renamed to *fresnelyc.m* to avoid ambiguity with a function introduced in MATLAB, Version R2014a.



## 2. Introduction

The growth and decay of the natural snowcover leads to characteristic stratification. The effects of snow metamorphosis typically cause the snow grain size, shape, density, and liquid water content to vary with time and from layer to layer. These changes in snow structure occur at characteristic time scales and often at characteristic dates during the lifetime of the snowcover, which thus contains key information on past conditions. Ground-based measurements have shown that the radiometric properties of snow are strongly affected by these parameters. Therefore we need a model to simulate these effects.

The need for such a model has been the motivation of modeling efforts since the 80's at the IAP. The basics of MEMLS were developed during an ESA study and published in several technical notes (Mätzler [1996b], Wiesmann and Mätzler [1997], Mätzler and Wiesmann [1997], Mätzler [1998]). The microwave behavior of single snow layers was investigated by Weise [1996] and later by Wiesmann *et al.* [1998]. The measurements of these authors lead to the empirical approach to determine the scattering coefficient of snow at a the frequency range of 5 to 100 GHz and a correlation length range of 0.05 to 0.3 mm (Wiesmann and Mätzler, 1999). In a further development in the same frequency range, the application was extended to coarse-grained snow with correlation lengths up to 0.6 mm (Mätzler And Wiesmann, 1999).

In MEMLS the snowcover is considered as a stack of horizontal layers. Each layer is characterized by thickness, correlation length, density, liquid water content and temperature. The layer interfaces are assumed as planar. In order to combine internal scattering and reflections at the interfaces, a sandwich model, based on multiple scattering radiative transfer, is used. Internal volume scattering is accounted for by a two-flux model (up and down welling streams) derived from a six-flux approach (fluxes in all space directions). However, the absorption and scattering coefficients are functions of the six-flux parameters. The absorption coefficient can be obtained from density, frequency and temperature, and the scattering coefficient depends on the correlation length, density and frequency Wiesmann *et al.* [1998].

In the first part of this paper the theoretical background of the model is presented. First it is shown how the snow brightness temperature  $T_b$  depends on the layer geometry and on the radiometric properties of each layer. Second the details are described.

In the second part a survey over the software implementation is given. The final section presents an example of a MEMLS simulation.

## 3. Microwave Emission Model of Layered Snowpack

The snowcover is assumed to be a stack of  $n$  horizontal snow layers ( $j = 1, 2, \dots, n$ ) with planar boundaries between air-snow and snow-snow (Figure 1) characterized by (for a given frequency  $f$ , polarization  $p$ , and incidence angle  $\theta = \theta_n$ )

- the snowpack brightness temperature  $T_b$ ,
- the reflectivity at the bottom of the snowpack  $s_0$  and the temperature at the bottom  $T_0$ ,
- the interface reflectivity on top of each layer  $s_j$ ,
- the internal reflectivity  $r_j$ , emissivity  $e_j$ , transmissivity  $t_j$  temperature  $T_j$  of each layer due to volume scattering and absorption. Energy conservation requires  $r_j + e_j + t_j = 1$ ,
- the downwelling (sky) radiation, given by the brightness temperature  $T_{sky}$ ,
- the layer thickness  $d_j$  and the number of layers  $n$ .

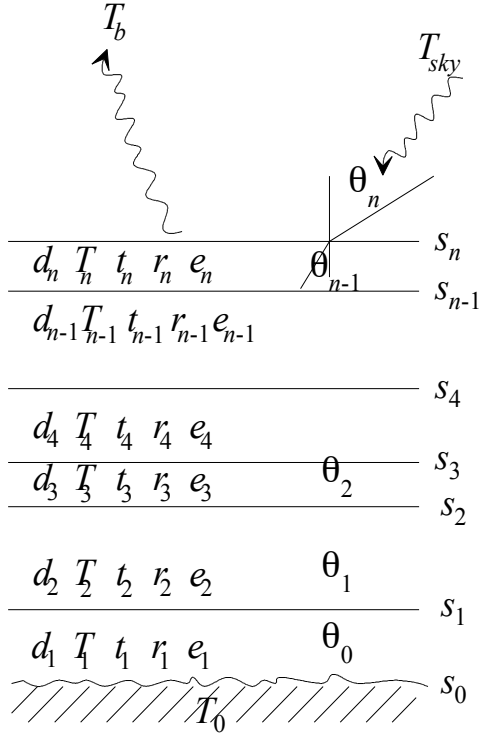


**Figure 1:** A multi layer system with a wave incident from above at an angle  $\theta_n$ .

The snow-ground interface is allowed to be rough; we only specify its reflectivity  $s_0$ , based on observation or theory. The presence of vegetation at the snow-ground interface is an interesting topic to be considered in the further development of MEMLS.

### 3.1 Radiation in multi-layered media

Considering Figure 2 we can derive the following equations relating the brightness temperatures at the boundaries:

$$A_j = r_j B_j + t_j C_j + e_j T_j \quad (1)$$

$$B_j = s_{j-1} A_j + (1 - s_{j-1}) D_{j-1} \quad (2)$$

$$C_j = (1 - s_j) A_{j+1} + s_j D_j \quad (3)$$

$$D_j = t_j B_j + r_j C_j + e_j T_j \quad (4)$$

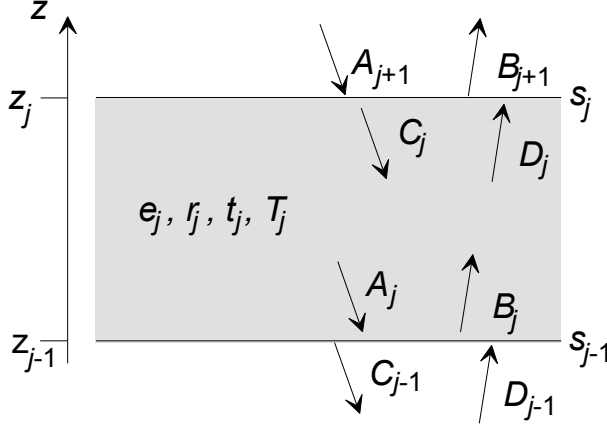


**Figure 2:** The parameters of a selected layer  $j$ .

where  $j$  runs from 1 to  $n$ . Note that for  $j = 1$  on the left-hand side of (2) we have a term with  $D_0$  on the right-hand side. It is given by the ground temperature

$$D_0 = T_0 \quad (5)$$

and  $s_0$  is the ground-snow reflectivity. Similarly for  $j = n$  we have in (3) a term with  $A_{n+1}$ , namely

$$A_{n+1} = T_{sky} \quad (6)$$

The brightness temperature  $B_{n+1} = T_b$  of the whole snowpack above the snowcover can be derived from

$$T_b = (1 - s_n)D_n + s_n T_{sky} \quad (7)$$

This is the main model result.

Sometimes the emissivity  $e_{sp}$  or the transmissivity  $t_{sp}$  of the whole snowpack is of more interest than the brightness temperature  $T_b$ . The computation of these parameters is not obtained by simply dividing  $T_b$  by a physical temperature because the snowpack is not regarded as isothermal. Nevertheless by computing  $T_b$  under various illumination conditions the required quantities can be found. As an example we can get the emissivity from two choices of  $T_{sky}$  (0K and 100K),

$$e_{sp} = 1 - \frac{T_b(T_{sky} = 100K) - T_b(T_{sky} = 0K)}{100K} \quad (8)$$

Likewise  $t_{sp}$  can be obtained from

$$t_{sp} = \frac{T_b(T_0 = 273K) - T_b(T_0 = 173K)}{100K(1 - s_0)} \quad (9)$$

$D_n$  can be derived from the system of linear equations (1) to (7) for  $j = 1$  to  $n$ . In order to solve these equations, we first eliminate the temperatures  $B_j$  and  $C_j$  in (1) and (4) by using (2) and (3). In this way we get a coupled system of linear equations for the temperatures  $A_j$  and  $D_j$ .

$$A_j = r_j [s_{j-1} A_j + (1 - s_{j-1}) D_{j-1}] + t_j [(1 - s_j) A_{j+1} + s_j D_j] + e_j T_j \quad (10)$$

$$D_j = t_j [s_{j-1} A_j + (1 - s_{j-1}) D_{j-1}] + r_j [(1 - s_j) A_{j+1} + s_j D_j] + e_j T_j \quad (11)$$

This system can be written in matrix and vector notation as

$$A = M_1 A + M_2 D + E \quad (12)$$

$$D = M_3 A + M_4 D + F \quad (13)$$

where  $A$  and  $D$  are the  $n$ -dimensional vectors containing the unknown brightness temperatures  $A_j$  and  $D_j$  ( $j = 1$  to  $n$ ), respectively,  $M_k$  ( $k = 1$  to  $4$ ) are  $n \times n$  matrices containing elements, defined by (10) and (11), and  $E$  and  $F$  are the vectors consisting of the known temperatures of each layer including the brightness of the sky and the ground temperature, i.e. the terms containing  $A_{n+1}$  and  $D_0$  in (10) and (11) which are not contained in the vectors  $A$  and  $D$ . Note that the non-zero values of the  $M_k$  are at and immediately next to the diagonal, since the indices of individual equations of (10) and (11) only vary from  $j - 1$  to  $j + 1$ .

In order to find  $D$  and thus  $D_n$  we can solve the system (12) and (13) by the rules of linear algebra, using matrix inversion. Here, the matrix inversions are not critical operations because the matrices to be inverted are far from being singular due to the concentration of large values on the diagonal. The result is:

$$D = (\mathbf{I} - M_5)^{-1} (M_3 (\mathbf{I} - M_1)^{-1} E + F) \quad (14)$$

where

$$M_5 = M_3 \left\{ (\mathbf{I} - M_1)^{-1} M_2 \right\} + M_4 \quad (15)$$

and where  $\mathbf{I}$  is the Identity Matrix. With (7) we get the final result from the last element  $D_n$  of the vector  $D$  to be computed with Equation (14).

### 3.2 The given matrices and vectors of the layered snowpack model

As an example we formulate the individual matrices and vectors for the case of 5 snow layers ( $n = 5$ ). The objects can easily be adapted for a different number of layers.

$$M_1 = \begin{pmatrix} r_1 s_0 & t_1(1-s_1) & 0 & 0 & 0 \\ 0 & r_2 s_1 & t_2(1-s_2) & 0 & 0 \\ 0 & 0 & r_3 s_2 & t_3(1-s_3) & 0 \\ 0 & 0 & 0 & r_4 s_3 & t_4(1-s_4) \\ 0 & 0 & 0 & 0 & r_5 s_4 \end{pmatrix}$$

$$M_2 = \begin{pmatrix} t_1 s_1 & 0 & 0 & 0 & 0 \\ r_2(1-s_1) & t_2 s_2 & 0 & 0 & 0 \\ 0 & r_3(1-s_2) & t_3 s_3 & 0 & 0 \\ 0 & 0 & r_4(1-s_3) & t_4 s_4 & 0 \\ 0 & 0 & 0 & r_5(1-s_4) & t_5 s_5 \end{pmatrix} \quad (16)$$

$$\begin{aligned}
M_3 &= \begin{pmatrix} t_1 s_0 & r_1(1-s_1) & 0 & 0 & 0 \\ 0 & t_2 s_1 & r_2(1-s_2) & 0 & 0 \\ 0 & 0 & t_3 s_2 & r_3(1-s_3) & 0 \\ 0 & 0 & 0 & t_4 s_3 & r_4(1-s_4) \\ 0 & 0 & 0 & 0 & t_5 s_4 \end{pmatrix} \\
M_4 &= \begin{pmatrix} r_1 s_1 & 0 & 0 & 0 & 0 \\ t_2(1-s_1) & r_2 s_2 & 0 & 0 & 0 \\ 0 & t_3(1-s_2) & r_3 s_3 & 0 & 0 \\ 0 & 0 & t_4(1-s_3) & r_4 s_4 & 0 \\ 0 & 0 & 0 & t_5(1-s_4) & r_5 s_5 \end{pmatrix} \\
E &= \begin{pmatrix} e_1 T_1 + r_1(1-s_0)T_0 \\ e_2 T_2 \\ e_3 T_3 \\ e_4 T_4 \\ e_5 T_5 + t_5(1-s_5)T_{sky} \end{pmatrix} ; \quad F = \begin{pmatrix} e_1 T_1 + t_1(1-s_0)T_0 \\ e_2 T_2 \\ e_3 T_3 \\ e_4 T_4 \\ e_5 T_5 + r_5(1-s_5)T_{sky} \end{pmatrix}
\end{aligned} \tag{17}$$

If only one layer is present, (14) is given by

$$D = D_1 = \frac{t_1 s_0 \frac{r_1(1-s_0)T_0 + t_1(1-s_1)T_{sky} + e_1 T_1}{1-r_1 s_0} + t_1(1-s_0)T_0 + r_1(1-s_1)T_{sky} + e_1 T_1}{1-r_1 s_1 - \frac{t_1^2 s_0 s_1}{1-r_1 s_0}} \tag{18}$$

### 3.3 Radiative transfer in snow - the six flux model

In order to compute realistic values of  $r_j$ ,  $e_j$ , and  $t_j$  for each layer the volume scattering and the absorption of each layer  $j$  has to be described by a radiative transfer model. An important distinction between radiative transfer in atmospheric radiation and the present situation is the fact that the mean refractive index of snow is significantly larger than unity. Refraction plays a role in snowpacks. But more important is the fact that total internal reflection occurs for certain rays. Our model takes these processes into account. We use a simplified radiative transfer model, reducing the radiation at a given polarization to six fluxes streaming along and opposed to the three principal axes of the slab (Figure 3). For simplification and because we look at one specific layer, the layer indices are mostly omitted.

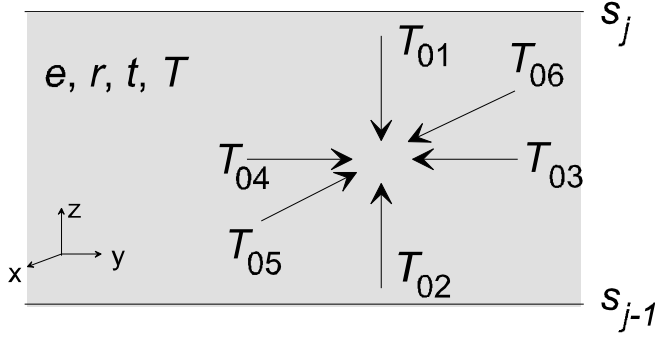


**Figure 3:** The parameters of a selected layer  $j$ .

It will be shown that in the case of a plane-parallel slab the model reduces to the well-known two-flux model where the absorption and scattering coefficients are functions of the six-flux parameters. The horizontal fluxes represent trapped radiation, that is, radiation whose internal incidence angle  $\theta$  is larger than the critical angle  $\theta_c$  for total reflection, where  $\theta_c$  is given by (19):

$$\theta > \theta_c = \arcsin(\sqrt{1/\varepsilon}) \quad (19)$$

where  $\varepsilon$  is the relative permittivity of the slab. The vertical fluxes represent the radiation which can escape from the snowpack, i.e. which does not undergo total reflection ( $\theta < \theta_c$ ). Considering the two-flux model alone would not allow us to include the trapping effect. Scattering by angles near  $90^\circ$  causes a coupling between the vertical and the horizontal fluxes. The trapped horizontal fluxes are represented by  $T_{03}$  to  $T_{06}$ . Radiation at  $\theta < \theta_c$  can be transmitted through the interface; thus its fluxes are represented by  $T_{01}$  for downwelling radiation and by  $T_{02}$  for upwelling radiation. Here we assume that the radiation of the vertical fluxes can be represented by an effective propagation direction represented by the angle  $\theta$  with respect to the  $z$  axis. Then the transfer equations for the six fluxes, expressed by brightness temperatures, are

$$-\frac{dT_{01}}{dz}|\cos\theta| = -\gamma_a(T_{01} - T) - \gamma_b(T_{01} - T_{02}) - \gamma_c(4T_{01} - T_{03} - T_{04} - T_{05} - T_{06}) \quad (20)$$

$$+\frac{dT_{02}}{dz}|\cos\theta| = -\gamma_a(T_{02} - T) - \gamma_b(T_{02} - T_{01}) - \gamma_c(4T_{02} - T_{03} - T_{04} - T_{05} - T_{06}) \quad (21)$$

$$-\frac{dT_{03}}{dx} = -\gamma_a(T_{03} - T) - \gamma_b(T_{03} - T_{04}) - \gamma_c(4T_{03} - T_{01} - T_{02} - T_{05} - T_{06}) \quad (22)$$

$$+\frac{dT_{04}}{dx} = -\gamma_a(T_{04} - T) - \gamma_b(T_{04} - T_{03}) - \gamma_c(4T_{04} - T_{01} - T_{02} - T_{05} - T_{06}) \quad (23)$$

$$-\frac{dT_{05}}{dy} = -\gamma_a(T_{05} - T) - \gamma_b(T_{05} - T_{06}) - \gamma_c(4T_{05} - T_{03} - T_{04} - T_{01} - T_{02}) \quad (24)$$

$$+\frac{dT_{06}}{dy} = -\gamma_a(T_{06} - T) - \gamma_b(T_{06} - T_{05}) - \gamma_c(4T_{06} - T_{03} - T_{04} - T_{01} - T_{02}) \quad (25)$$

where  $\gamma_a$  is the absorption coefficient,  $\gamma_b$  the scattering coefficient in the backward direction and  $\gamma_c$  the scattering coefficient for scattering by about  $90^\circ$ . We assume that the medium is plane parallel and isotropic in the  $(x, y)$  plane, so that the fluxes  $T_{03}$  to  $T_{06}$  are the same, with vanishing derivatives in  $x$  and  $y$  directions, leading to

$$T_{03} = T_{04} = T_{05} = T_{06} = (\gamma_a T + \gamma_c(T_{01} + T_{02}))(\gamma_a + 2\gamma_c)^{-1} \quad (26)$$



Inserting (26) in (20) and (21) leads to two-flux equations with modified coefficients:

$$-\frac{dT_{01}}{dz}|\cos\theta| = -\gamma'_a(T_{01} - T) - \gamma'_b(T_{01} - T_{02}) \quad (27)$$

$$+\frac{dT_{02}}{dz}|\cos\theta| = -\gamma'_a(T_{02} - T) - \gamma'_b(T_{02} - T_{01}) \quad (28)$$

The two-flux absorption coefficient  $\gamma'_a$  and scattering coefficient  $\gamma'_s$  can be written in terms of the six-flux parameters:

$$\gamma'_a = \gamma_a \left( 1 + 4\gamma_c (\gamma_a + 2\gamma_c)^{-1} \right) \quad (29)$$

$$\gamma'_b = \gamma_b + 4\gamma_c^2 (\gamma_a + 2\gamma_c)^{-1} \quad (30)$$

For constant  $T$  and constant coefficients,  $T_{01}$  and  $T_{02}$  can be written as

$$T_{01} = T + A \exp(\gamma d') + B \exp(-\gamma d') \quad (31)$$

$$T_{02} = T + r_0 A \exp(\gamma d') + r_0^{-1} B \exp(-\gamma d') \quad (32)$$

where

$$d' = d/|\cos\theta|. \quad (33)$$

An «effective incidence angle»  $\theta$  (see below, especially (59)) is assumed for the vertical fluxes.

The reflectivity  $r_0$  at infinite slab thickness is given by

$$r_0 = \gamma'_b (\gamma'_a + \gamma'_b + \gamma)^{-1} \quad (34)$$

and the damping coefficient  $\gamma$  is given by

$$\gamma = \sqrt{\gamma'_a (\gamma'_a + 2\gamma'_b)} \quad (35)$$

For a snow layer of thickness  $d$  the values for the internal  $r$  and  $t$  considering all multiple reflections are

$$r = r_0 (1 - t_0^2) (1 - r_0^2 t_0^2)^{-1} \quad (36)$$

$$t = t_0 (1 - r_0^2) (1 - r_0^2 t_0^2)^{-1} \quad (37)$$

where

$$t_0 = \exp(-\gamma d') \quad (38)$$

is the one-way transmissivity through the slab.

Only in the case of a known relationship between  $\gamma_b$  and  $\gamma_c$  are we able to derive all parameters of the six-flux model. The way  $\gamma_b$  and  $\gamma_c$  are related is determined by the internal scattering phase function and by the critical angle  $\theta_c$  given by (19). The solid angle of the beams for  $T_{01}$  and  $T_{02}$  is

$$\Omega_1 = 2\pi \left( 1 - \sqrt{\frac{\epsilon - 1}{\epsilon}} \right) \quad (39)$$

and the solid angle  $\Omega_2$  of trapped radiation is the complement  $2\pi - \Omega_1$ ; that is,

$$\Omega_2 = 2\pi \sqrt{\frac{\epsilon - 1}{\epsilon}} \quad (40)$$

Furthermore, for volume scattering consisting of a specular component  $\gamma_{b0}$  and of a diffuse term  $\gamma_{b1}$  such that

$$\gamma_b = \gamma_{b0} + \gamma_{b1} \quad (41)$$

the diffuse scattering coefficient  $\gamma_s$  is

$$\gamma_s = 2\gamma_{b1} + 4\gamma_c \quad (42)$$

and using (39) and (40) we get for isotropy of diffuse scattering

$$\frac{2\gamma_c}{\gamma_{b1}} = \frac{\Omega_2}{\Omega_1} \quad (43)$$

Due to the Brewster effect, the specular term  $\gamma_{b0}$  is very sensitive to polarization, whereas this is not the case for  $\gamma_{b1}$ . Assuming that we can separate these two parameters, we are then able to determine the six-flux coefficients. With equations (39) - (43) we can determine the six-flux coefficients  $\gamma_a$ ,  $\gamma_b$ ,  $\gamma_c$  and  $\gamma_s$ <sup>i</sup> from the snow permittivity  $\epsilon$  and from the two-flux coefficients  $\gamma_a'$  and  $\gamma_b'$ , using (29) and (30). So far in all our computations the term  $\gamma_{b0}$  has been set to  $\gamma_{b0} = 0$ ; i.e.  $\gamma_b = \gamma_{b1}$ .

### 3.4 Reflectivity at layer interfaces

The interface reflectivity  $s_j$  between two regular layers is given by the Fresnel formula ( $s_j = |F_j|^2$ ;  $F_j$  is the Fresnel reflection coefficient):

$$s_j = \left( \frac{\sqrt{\epsilon_{j+1}} \cos \theta_j - \sqrt{\epsilon_j - \epsilon_{j+1} \sin^2 \theta_j}}{\sqrt{\epsilon_{j+1}} \cos \theta_j + \sqrt{\epsilon_j - \epsilon_{j+1} \sin^2 \theta_j}} \right)^2 ; \text{ h-pol} \quad (44)$$

$$s_j = \left( \frac{\epsilon_j \cos \theta_j - \sqrt{\epsilon_{j+1}} \sqrt{\epsilon_j - \epsilon_{j+1} \sin^2 \theta_j}}{\epsilon_j \cos \theta_j + \sqrt{\epsilon_{j+1}} \sqrt{\epsilon_j - \epsilon_{j+1} \sin^2 \theta_j}} \right)^2 ; \text{ v-pol} \quad (45)$$

By regular we mean that a simple transition occurs in the permittivities  $\epsilon_j$  to  $\epsilon_{j+1}$ , and that coherent superpositions due to reflections at other interfaces can be ignored.

#### *Reflectivity on a thin layer*

For layers thinner than  $\lambda/2$  the coherent reflection dominates the microwave behavior. Strong coherent effects are expected for layers of the size  $\lambda/4$  (see Figure 5). Due to the spatial variability in the thickness of layers, the coherent effects are smeared out for thicker layers by averaging over lateral distances, and also by averaging over the beamwidth and bandwidth of the radiometers; then the coherent effects disappear, and thus they can be ignored.

According to the invariant embedding method by *Adams and Denman* [1966] the coherent reflection coefficient  $R_n$  of a system containing  $n$  coherent layers (Figure 1) can be written as:

$$R_n = \frac{F_n + R_{n-1} e^{2iP_n}}{1 + F_n R_{n-1} e^{2iP_n}} ; n \geq 1 \quad (46)$$

where  $F_n$  is the Fresnel reflection coefficient for the interface between layer  $n$  and  $n+1$ ,  $R_{n-1}$  is the reflection coefficient for the system containing  $n-1$  layers ( $R_0 = F_0$ ) and  $P_j$  is the one-way phase through layer  $j$  (here for  $j = n$ ), given by

<sup>i</sup> In the present version of MEMLS we set  $\gamma_{b0} = 0$ , i.e. the specular reflection terms are exclusively assumed to occur at layer interfaces.

$$P_j = \frac{2\pi d_j n_j \cos \theta_{j-1}}{\lambda}. \quad (47)$$

which is a function of the thickness  $d_j$ , of layer  $j$ , the refractive index  $n_j$ , the propagation angle  $\theta_j$  and the vacuum wavelength  $\lambda$ .

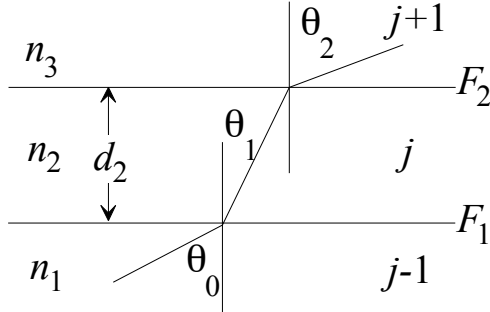


**Figure 4:** Thin layer  $j$  of coherent reflection between two scattering layers  $j-1$  and  $j+1$ , here for  $j=2$ .

To simplify (46) we define

$$E_j \equiv e^{2ip_j}. \quad (48)$$

Using (46) and (48) the reflection coefficient of a double layer (Figure 4)  $R_2$  (with  $R_1 = F_1$ ) can be written as

$$R_2 = \frac{F_2 + F_1 E_2}{1 + F_2 F_1 E_2} \quad (49)$$

The power reflectivity  $s$  of a double layer is given by

$$s = |R_2|^2 = \left| \frac{F_2 + F_1 E_2}{1 + F_2 F_1 E_2} \right|^2. \quad (50)$$

If the interface reflection coefficients are real and  $P_2 = P_2' + iP_2''$  then

$$s = \frac{F_2^2 + F_1^2 e^{-4P_2''} + 2F_1 F_2 e^{-2P_2''} \cos(2P_2')}{1 + F_1^2 F_2^2 e^{-4P_2''} + 2F_1 F_2 e^{-2P_2''} \cos(2P_2')} \quad (51)$$

and

$$2P_2' = \frac{4\pi d_2 n_2' \cos \theta_1}{\lambda} \quad (52)$$

$$2P_2'' = \frac{4\pi d_2 n_2''}{\lambda \cos \theta_1}. \quad (53)$$

If  $P_2'' \ll 1$ , then (51) simplifies to

$$s = \frac{F_2^2 + F_1^2 + 2F_1 F_2 \cos(2P_2')}{1 + F_1^2 F_2^2 + 2F_1 F_2 \cos(2P_2')} \quad (54)$$

and

$$2P_2 = \frac{4\pi d_2 n_2' \cos \theta_1}{\lambda}. \quad (55)$$

The coherent power reflectivity  $s$  of a thin layer  $j$  depends on  $d_j$  by a cosine function  $\cos(2P_j)$ :

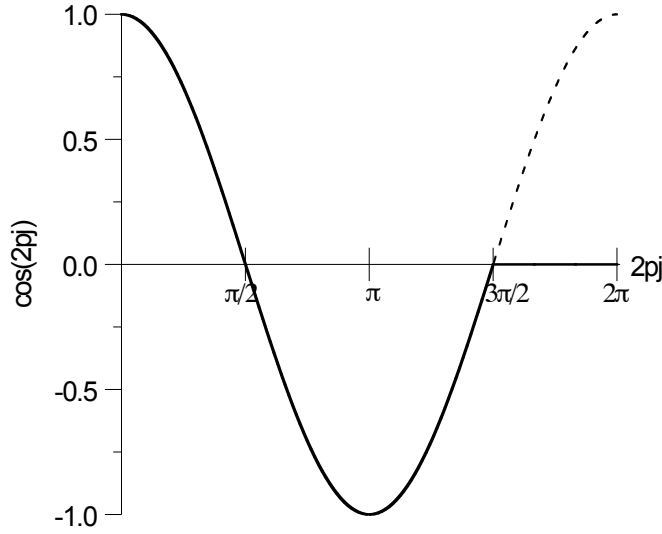


**Figure 5:** Dependence of  $s$  with  $d$ :  $\cos(2P_j)$  as a function of  $2P_j$ . The thick solid line shows the part of the coherent phase term that is taken into account in MEMLS.

Figure 5 presents  $\cos(2P_j)$  as a function of  $2P_j$ . It is useful to handle a layer as coherent as long as  $2P_j < 3\pi/2$ . I.e. a layer is defined as thin and handled as a coherent layer if

$$2P_j < 3\pi/2 \approx 4.7. \quad (56)$$

Otherwise the layer is considered as incoherent (see Section 3.3); especially the interface reflectivity is given by  $s_j = |F_j|^2$ . Condition (56), and using (55) with  $j = 2$  ensures that the  $d_j$  of the coherently reflecting slab is less than about half a wavelength.

The effect of the coherent layer  $j$  is taken into account by using the coherent reflectivity  $s$  of the thin layer as the interface reflectivity  $s_j$  between the two scattering layers,  $j+1$  and  $j-1$ , separated by the thin layer. Afterwards the coherent layer is removed from the input table of the layered snowpack emission model, i.e. the coherent layer is represented exclusively by  $s$ . Note that this procedure has to be done for each frequency and incidence angle.

Some restrictions apply. The snowpack emission model works only if there is at least one scattering layer, i.e. one regular layer. Because coherent interaction with a rough ground surface cannot be described within our model, it is also required that the lowest snow layer is incoherent. However, a coherent surface layer is allowed by the model. In this case, the top layer in (Figure 4) is the air above the snow surface.

### 3.5 Effective propagation angle and polarization effects

In the previous sections a model for microwave emission of a  $n$ -layer snowpack was presented. The model is based on a simplified radiative transfer, described by six "fluxes" streaming along and against the principal axes. It was assumed that the effective propagation angle  $\theta_j$  with respect to the surface normal is given by Snell's law of refraction at any position of the snowpack for both vertically and horizontally polarized radiation. Horizontal snow layers with smooth interfaces are assumed throughout the model. Deviations in propagation direction occur due to diffuse volume scattering. This does not necessarily mean that the effective propagation angle of the fluxes changes. Especially for an incidence angle near 50 degrees the effective propagation angle is similar to the one computed from Snell's law. However at near vertical incidence scattering leads to an increase of the effective propagation angle making it necessary to correct this angle. The enhancement proposed is a first- order correction in effective

propagation path and polarization mixing, considering single-scattering of radiation originating at the radiometer antenna and propagating into the snowpack (i.e. we describe the reciprocal and equivalent path of photons as if they were emitted by the radiometer antenna).

The consequences of a modified propagation angle are

- a different length of the propagation path within each snow layer, leading to a modified transmissivity, see (33) and (38).
- change of the effective reflectivities at layer interfaces at v and h polarization.

### **Effective propagation angle**

For a radiometer observing at the incidence angle  $\theta_n$  the effective propagation angle inside the snowpack is well approximated by  $\theta_{js}$  as determined by Snell's law of refraction,

$$\sin\theta_{js} = \sin\theta_n / n'_{j+1} ; j=n-1, n-2, \dots, 1, 0 \quad (57a)$$

(Index  $s$  standing for 'Snell') for smooth and horizontal surfaces and layer interfaces as long as volume scattering is not too important. This is true at least just below the snow surface. However, with increasing snow depth, more and more of the forward streaming flux consists of forward scattered radiation leading to an effective propagation angle that differs from  $\theta_{js}$ .

Assuming that, in the limit of strong scattering, the forward (downward) and backward (upward) fluxes are isotropic (or **diffuse**) then the effective propagation angle  $\theta_{jd}$  can be represented by

$$\cos\theta_{jd} = \frac{1 + \cos\theta_{jc}}{2} \quad (57b)$$

where  $\theta_{jc}$  is the **critical** angle for total reflection, i.e. the maximum propagation angle of radiation belonging to the vertical fluxes; it is given by

$$\cos\theta_{jc} = \sqrt{1 - (n'_{j+1})^{-2}} \quad (58)$$

For a diluted medium where  $n_j = 1$  we get  $\cos\theta_{jd} = 0.5$ ; this is the usual value of the two-stream model *Ishimaru* [1978]. In our case of six streams or "fluxes", the streams have more narrow beams, therefore we have to use the modified form given by Equation (57b).

The actual value of the effective propagation angle  $\theta_j$  in layer  $j+1$  is somewhere between  $\theta_{js}$  and  $\theta_{jd}$ . We assume that the two cosines are weighted according to the transmissivity of  $t_z$  for non-scattered radiation from the snow surface (at height  $z_{j+1}$ ) to height  $z < z_{j+1}$ , i.e.

$$\cos\theta_j = t_z \cos\theta_{js} + (1 - t_z) \cos\theta_{jd} \quad (59)$$

and  $t_z$  is given by

$$t_z = \exp\left(-\int_z^{z_{j+1}} \frac{\gamma_s(z')}{\cos\theta_{js}} dz'\right) \quad (60)$$

where  $\gamma_s(z')$  is the scattering coefficient at height  $z'$ . For negligible scattering  $t_z \Rightarrow 1$ , leading to  $\theta_j = \theta_{js}$ , whereas for strong scattering we get  $t_z = 0$  and thus  $\theta_j = \theta_{jd}$ . In the snowpack model the effective incidence angle is changed only at the layer interface, assuming constant values within each layer. Thus the value of  $z$  in Equation (60) is limited to  $z_j; j = 1, 2, \dots, n$ .

### **Polarization mixing**

After diffuse scattering the photons loose their memory about where they came from. As a consequence they cannot remember their plane of incidence which is needed to define the state of h or v polarization. Therefore the v- and h-polarized fluxes are mixed in a similar way as  $\theta_{js}$  and  $\theta_{jd}$ . This mixing can be modeled by modifying the polarization-dependent parts of the

snowpack model, i.e. the reflectivities  $s_{jv}$  and  $s_{jh}$  at the interface between Layer  $j$  and  $j+1$ . The computation of these reflectivities without polarization mixing is described in Section 3.4. Here we estimate the modification due to the mixing effect. Let us denote the difference  $\Delta s_j$  by

$$\Delta s_j = s_{jh} - s_{jv} \quad (61)$$

This difference is reduced due to scattering, leading to effective interface reflectivities  $s_{jveff}$  and  $s_{jheff}$  between Layer  $j$  and  $j+1$  at position  $z = z_j$ :

$$s_{jheff} = 0.5 \left[ s_{jh} + s_{jv} + t_z \Delta s_j \right] \quad (62)$$

$$s_{jveff} = 0.5 \left[ s_{jh} + s_{jv} - t_z \Delta s_j \right] \quad (63)$$

In (62) and (63) the values of  $s_{jv}$  and  $s_{jh}$  are the ones computed for the angles  $\theta_{js}$ . In a further improvement, these coefficients could be taken at the effective incidence angle  $\theta_j$ . However the effects of such a further correction are small because they tend to cancel. A more precise description of polarization mixing would require a fully polarimetric radiative transfer method.

### 3.6 Primary input parameters

At a given frequency  $f$ , polarization  $p$  and observation incidence angle  $\theta_n$  the following snow physical parameters are needed for each layer  $j$  ( $j = 1, \dots, n$ ):

- density  $\rho_j$
- temperature  $T_j$
- salinity  $Sppt$
- liquid water content  $W_j$
- correlation length  $p_{cj}$
- vertical extent  $z_j$
- physical ground temperature  $T_0$
- snow-ground reflectivity  $s_0$

These primary parameters define the derived secondary model parameters to be described below.

### 3.7 Secondary model parameters

#### *Dielectric properties of dry snow*

For dry snow the microwave permittivity can be expressed according to *Mätzler* [1996] in terms of the density  $\rho$  in  $\text{g/cm}^3$ :

$$\epsilon'_d = 1 + 1.5995\rho + 1.861\rho^3; \quad 0 \leq \rho \leq 0.4 \text{ g/cm}^3 \quad (64)$$

$$\epsilon'_d = \left( (1 - v)\epsilon_h + v\epsilon_s \right)^3; \quad \rho > 0.4 \text{ g/cm}^3 \quad (65)$$

where  $\epsilon_h = 1.0$ ,  $\epsilon_s = 1.4759$  and  $v = \rho/0.917 \text{ g/cm}^3$ .

The imaginary part of the dielectric constant of dry snow is given by:

$$\epsilon''_d = \sqrt{\epsilon'_d} K^2 v \epsilon''_i \quad (66)$$

where  $K^2$  is the field factor [*Mätzler*, 1998a]. Its value is near 0.5. In the subroutine it is also possible to choose  $\epsilon''$  as proposed by *Tiuri et al.* [1984].

$$\varepsilon_d'' = \varepsilon_i''(0.52 \cdot \rho + 0.62 \cdot \rho^2) \quad (67)$$

The complex part of the dielectric permittivity of ice is determined from *Mätzler et al* [2006]

$$\varepsilon_i'' = \frac{\alpha}{f} + \beta \cdot f \quad (68)$$

$$\theta = \frac{300K}{T} - 1 \quad (69)$$

$$\alpha = (0.00504 + 0.0062 \cdot \theta) \cdot \exp(-22.1 \cdot \theta) \quad (70)$$

$$\beta = \frac{B_1}{T} \cdot \frac{\exp(b/T)}{(\exp(b/T) - 1)^2} + B_2 f^2 + \exp(-9.963 + 0.0372 \cdot (T - 273.16K)) \quad (71)$$

where  $T$  is the temperature in K,  $f$  is the frequency in Gigahertz,  $B_1 = 0.0207 \text{ K GHz}^{-1}$ ,  $b = 335 \text{ K}$  and  $B_2 = 1.16 \cdot 10^{-11} \text{ GHz}^{-3}$ .

For saline ice the losses of ice are larger. Measurements for slightly saline ice, found in snow on sea ice, indicated the following behavior

$$\varepsilon_{is}'' = \varepsilon_i'' + \Delta\varepsilon_i'' S/S_0$$

where  $S$  is the salinity,  $S_0 = 0.013$  parts per thousand, and

$1/\Delta\varepsilon_i'' = g_0 + g_1 (273.16 - T)$ . The parameters  $g_0$  and  $g_1$  depend on frequency (here in GHz) and are given by

$$g_0 = 1866 \exp(-0.317 f); \quad g_1 = 72.2 + 6.02 f$$

The real part of the dielectric permittivity of dry snow is assumed to be frequency independent.

### ***Dielectric properties of wet snow***

In contrast, wet snow exhibits a distinct Debye relaxation spectrum in the microwave range. According to the physical mixing model of *Mätzler* [1987] for small values of  $W$  (volumetric liquid water content), the microwave permittivity  $\varepsilon = \varepsilon' + i\varepsilon''$  is given by

$$\varepsilon = \varepsilon_a + \varepsilon_b + \varepsilon_c + \varepsilon_d \quad (72)$$

where  $\varepsilon_d$  is the permittivity of dry snow. The terms  $\varepsilon_a$ ,  $\varepsilon_b$ ,  $\varepsilon_c$  are Debye terms expressed as

$$\varepsilon_k = \varepsilon_{\infty k} + \frac{\varepsilon_{sk} - \varepsilon_{\infty k}}{1 - if / f_{0k}}; \quad k = a, b, c \quad (73)$$

The Debye parameters  $\varepsilon_{sk}$ ,  $\varepsilon_{\infty k}$ ,  $f_{0k}$  are given by the following three relations

$$\varepsilon_{sk} = \frac{W}{3} \frac{\varepsilon_{sw} - \varepsilon_d}{1 + A_k \cdot \left( \frac{\varepsilon_{sw}}{\varepsilon_d} - 1 \right)}; \quad k = a, b, c \quad (74)$$

$$\varepsilon_{\infty k} = \frac{W}{3} \frac{\varepsilon_{\infty w} - \varepsilon_d}{1 + A_k \cdot \left( \frac{\varepsilon_{\infty w}}{\varepsilon_d} - 1 \right)}; \quad k = a, b, c \quad (75)$$

$$f_{0k} = f_{0w} \left[ 1 + \frac{A_k (\varepsilon_{sw} - \varepsilon_{\infty w})}{\varepsilon_d + A_k \cdot (\varepsilon_{\infty w} - \varepsilon_d)} \right]; \quad k = a, b, c \quad (76)$$

where the static permittivity  $\varepsilon_{sw}$ , the optical permittivity  $\varepsilon_{\infty w}$  and the relaxation frequency  $f_{0w}$  of liquid water at  $T = 0^\circ\text{C}$  are chosen ( $\varepsilon_{sw} = 88$ ,  $\varepsilon_{\infty w} = 4.9$ ,  $f_{0w} = 9 \text{ GHz}$  [*Ulaby et al.* 1986]). The depolarization factors are chosen according to *Mätzler* [1987]:  $A_a = 0.005$ ,  $A_b = A_c = 0.4975$ ,

based on measurements by *Hallikainen et al.* [1986] and by *Mätzler et al.* [1984]. Equation (76) for the relaxation frequency includes a correction of the original form given by *Mätzler* [1987]. Instead of the above formulas, in Version 3 of MEMLS, we introduced wet snow as a two-component mixture where the host  $\varepsilon_1$  is dry snow and the inclusion  $\varepsilon_2$  is pure water. The mixing formula of Maxwell Garnett

$$\varepsilon = \frac{(1-f)\varepsilon_1 + f\varepsilon_2 K}{1-f+fK}; K = \frac{1}{3}(K_a + K_b + K_c); K_i = \frac{\varepsilon_1}{\varepsilon_1 + A_i(\varepsilon_2 - \varepsilon_1)}$$

with spheroidal inclusions given by the above depolarization factors was chosen, and for the dielectric constant of water we used the formula of Liebe et al. (1991) with two relaxation frequencies.

### **Absorption coefficient**

The absorption coefficient  $\gamma_a$  ( $\varepsilon'' \ll \varepsilon'$ ) is given by

$$\gamma_a = \frac{2 \cdot \pi \cdot \varepsilon''}{\lambda_0 \cdot \sqrt{\varepsilon'}} \quad (77)$$

where  $\lambda_0$  is the vacuum wavelength and  $\varepsilon = \varepsilon' + i\varepsilon''$  is the complex permittivity of the medium. Using Equations (64) to (71),  $\gamma_a$  can be written as a function of snow density  $\rho$  and snow temperature  $T$  in K.

## **3.8 Tertiary model parameters**

### **Scattering coefficient**

According to *Wiesmann et al.* [1998] the scattering coefficient can be obtained from snow physical properties. In MEMLS different fits to the same experimental data are provided:

$$\gamma_s = 136 \left( \frac{p_c}{1 \text{ mm}} \right)^{2.85} \left( \frac{f}{50 \text{ GHz}} \right)^{2.5} \left( \frac{\rho}{\text{g/cm}^3} + 0.001 \right)^{-1} \quad (78)$$

$$\gamma_s = 3.16 \frac{p_{ec}}{1 \text{ mm}} + 295 (p_{ec})^{2.5} \left( \frac{f}{50 \text{ GHz}} \right)^{2.5} \quad (79)$$

$$\gamma_s = \left( 9.2 \frac{p_{ec}}{1 \text{ mm}} - 1.23 \frac{\rho}{\text{g/cm}^3} + 0.54 \right)^{2.5} \left( \frac{f}{50 \text{ GHz}} \right)^{2.5} \quad (80)$$

where  $p_c$  is the ‘slope’ correlation length and  $p_{ec}$  is the exponential correlation length, i.e. a correlation length obtained by fitting the measured correlation function to  $\exp(-x/p_{ec})$ . Best results were obtained with (80).

### **Other tertiary model parameters**

- interface reflectivity  $s_j$  : see Sections 3.4, 3.5
- layer reflectivity  $r_j$  : see Section 3.3
- layer transmissivity  $t_j$  : see Section 3.3
- layer emissivity  $e_j$  : see Section 3.3
- effective propagation angle and polarization mixing according to Section 3.5



## 4. Implementation

MEMLS is written in MATLAB 5 [MathWorks, 1996]. All subroutines are commented, and a help text is available with *help subroutine*. Below are some general remarks to each subroutine and to the references. With the subroutines *fmain* and *lmain* the brightness temperature versus incidence angle and frequency, respectively, of a given snowpack can be computed. These two programs shall illustrate in which order the subroutines must be used. The main program is *memlsmain*. The main input parameters are contained in the input ascii file where each line contains the data of one snow layer, with the top line representing the bottom layer just above the ground, and the bottom line representing the top snow layer:

Each line (layer) contains the following 7 input data:

Layer no.,  
Layer temperature (K),  
volumetric liquid-water content (vol. fraction): 0-1  
snow density (kg/m<sup>3</sup>)  
Layer thickness (cm)  
Snow salinity (parts per thousand)  
Exponential correlation length (mm)

As an example try 'memlsmain(21, 50, 0, 0, 'test1layer.txt', 0, 273, 11)'

### 4.1 The main routines and subroutines

#### *memlsmain*

```
function result = memlsmain(fGHz,tetad,s0h,s0v,ifile,Tsky,Tgnd,sccho)
% Basic MEMLS program, computes the brightness temperatures Tv and Th
% of a snowpack at a given frequency and incidence angle.
%   fGHz:    frequency [GHz]
%   tetad:   incidence angle [deg]
%   s0h:     snow-ground reflectivity, h-pol
%   s0v:     snow-ground reflectivity, v-pol
%   ifile:   Snowpack-Input File (ascii) with
% layer-number, temp [K], volume fraction of liquid water, density [kg/m3],
% thickness [cm], Salinity (0 - 0.1) [ppt], expon.corr.length [mm]
%   Tsky:    sky brightness temperature [K]
%   Tgnd:    ground temperature [K]
%   sccho:   type of scattering coefficient (11 recommended)
% Version history:
%   3.0      ma 02.04.2007
%   3.1      ma 05.04.2007 adapted to saline snow
% Uses:
%   vK2eps, epswet, epsaliceimag, pfadi, pfadc, polmix, fresnelyc,
%   slred, sccoeff, rt, layer
% Copyright (c) 2007 by the Institute of Applied Physics,
% University of Bern, Switzerland
% Aux. input parameter:
graintype=1;    % 1, 2 or 3 for different assumptions:
%"1" empirical snow measurements, "2" spheres, "3" thin shells
output: result=[Tbv,Tbh];
```

#### *fmain2*

```
function result=fmain2(freq,tetal,teta2,s0h,s0v,ifile,Tgnd,sccho)
% MEMLS program, plots and lists the incidence angle(deg), emissivities
% eh(%), ev(%), the emitted brightness temperatures Tebh(K), Tebv(K),
% and the effective physical temperatures Teffh(K), Teffv(K)
% of the emitting surface (ground and snowpack) of a layered snowpack.
```

```

%      fGHz:   frequency [GHz]
%      teta1:  start inc. angle [deg]
%      teta2:  stop incidence angle [deg]
%      s0h:    snow-ground reflectivity
%      s0v:    snow-ground reflectivity
%      ifile:  Snowpack-Input File with
% layer-number, temp [K], vol. fraction of liquid water, density [kg/m3],
% thickness [cm], Salinity (0 - 0.1) [ppt], expon.corr.length [mm]
%      Tgnd:   ground temperature [K]
%      sccho:  type of scattering coefficient (11 recommended)
% Version history:
%      3.0    ma 04.04.2007 adapted from fmain
%      3.1    ma 05.04.2007 adapted to saline snow
% Uses:
%      vK2eps, epswet, epsaliceimag, pfadi, pfadc, polmix, fresnelyc,
%      slred, sccoeff, rt, layer
% Copyright (c) 2007 by the Institute of Applied Physics,
% University of Bern, Switzerland
% Aux. input parameter:
graintype=1; % 1, 2 or 3 as in memlsmain:
result=[x',yh',yv',yeh',yev',yeh'./yh',yev'./yv'];
% Incidence angle(deg), eh(%), ev(%), Tebh(K), Tebv(K), Teffh(K), Teffv(K)

```

## *lmain2*

```

function result = lmain2(f1,f2,tetad,s0h,s0v,ifile,Tgnd,sccho)
% MEMLS main program, plots and lists the frequencies(GHz), emissivities
% eh(%), ev(%), the emitted brightness temperatures Tebh(K), Tebv(K),
% and the effective physical temperatures Teffh(K), Teffv(K)
% of the emitting surface (ground and snowpack) of a layered snowpack.
%      f1:     start frequency [GHz]
%      f2:     stop frequency [GHz]
%      tetad:  incidence angle [deg]
%      s0h:    snow-ground reflectivity
%      s0v:    snow-ground reflectivity
%      ifile:  Snowpack-Input File with
% layer-number, temp [K], vol. fraction of liquid water, density [kg/m3],
% thickness [cm], Salinity (0 - 0.1) [ppt], expon.corr.length [mm]
%      Tgnd:   ground temperature [K]
%      sccho:  type of scattering coefficient (11 recommended)
%
% Version history:
%      3.0    ma 04.04.2007 adapted from lmain
%      3.1    ma 05.04.2007 adapted to saline snow
% Uses:
%      vK2eps, epswet, epsaliceimag, pfadi, pfadc, polmix, fresnelyc,
%      slred, sccoeff, rt, layer
% Copyright (c) 2007 by the Institute of Applied Physics,
% University of Bern, Switzerland
% Aux. input parameter:
graintype=1; % 1, 2 or 3 as in memlsmain
result=[x',yh',yv',yeh',yev',yeh'./yh',yev'./yv'];
% Frequency(GHz), eh(%), ev(%), Tebh(K), Tebv(K), Teffh(K), Teffv(K)

```

## *borna*

```

function [gb6,gc6,gf6,gs6] = borna(k0,vfi,pci,epsi,eice,kq)
% calculates the scattering coefficient using Born Approximation
% [gb6,gc6,gf6,gs6] = borna(k0,vfi,pci,epsi,eice,kq)
%      gb6: 6-flux back scattering coefficient
%      gc6: 6-flux cross scattering coefficient
%      gf6: 6-flux forward scattering coefficient
%      gs6: 6-flux scattering coefficient
%      k0:   vacuum wave number (1/m)

```

```

%      vfi: volume fraction of ice
%      pci: correlation length (mm)
%      epsi: real dielectric constant of snow
%      eice: real dielectric constant of ice
%      kq : squared E-field ratio (from bornsnk)
% Version history:
%      1.0      wi 27.05.98,
%      3.0      lb 2.3.2007, 3.1 cm 2.4.2007
% Uses: integrmui
% Copyright (c) 2007 by the Institute of Applied Physics,
% University of Bern, Switzerland

```

### *epsr*

Calculates the dielectric permittivity  $\epsilon'$  of dry snow from snow density  $\rho$ . For  $\rho$  smaller or equal  $400 \text{ kg/m}^3$  (64) is used. For denser snow *Looyenga's* [1965] formula is used (65).

### *epsaliceimag*

```

function z = epsaliceimag(fGHz,TK,Sppt)
% MATLAB Function for calculating the imaginary part of the
% relative permittivity of pure ice in the microwave region,
% according to C. Matzler, IET Book (2006), chapter on ice
% Input:
% TK = temperature (K), range 20 to 273.15
% fGHz = frequency in GHz
% Sppt = salinity in parts per thousand

```

### *epsaliceimag*

```

function z = epsicereal(TK)
% Function for calculating the real relative permittivity
% of pure ice in the microwave region, according to
% Matzler, C.(ed),"Thermal Microwave Radiation - Applications for Remote
% Sensing", IET, London, UK (2006), Chapter 5.
% Input:
% TK = temperature (K), range 240 to 273.15
z = 3.1884 + 9.1e-4*(TK-273);

```

### *epswet*

```

function result = epswet(f,Ti,Wi,epsd);
% calculates complex dielectric constant of wet snow
% using Maxwell-Garnett Mixing rule of water in dry snow
% for prolate spheroidal water with experimentally determined
% depolarisation factors.
% Water temperature is at 273.15 K, with epsilon
% of water from Liebe et al. 1991.
%      epsd: complex epsilon of dry snow
%      f: frequency [GHz]
%      Ti: physical snow temperature [K]
%      Wi: wetness [volume fraction]
% Version history:
%      1.0      wi 15.7.95
%      2.0      ma 31.5.2005: Wi is volume fraction (not %)
%      3.0      ma 2.4.2007 : adjustments, new function name
% Uses: epswater (since Version 3)
% Copyright (c) 1997 by the Institute of Applied Physics,
% University of Bern, Switzerland

```

### *fresnelyc*

calculates the interface reflectivity  $s_h$ ,  $s_v$  of the snow slabs (using Fresnel) neglecting the imaginary part of the dielectric properties of snow  $\epsilon'' = 0$ .

### ***fresnelrc***

calculates the interface reflection coefficients  $F_h$ ,  $F_v$  of the snow slabs (after Fresnel) neglecting the imaginary part of the dielectric properties of snow  $\epsilon'' = 0$ .

### ***layer***

calculates the array D, see Equation (14), from the layer reflectivities  $r_j$  and transmissivities  $t_j$ , interface reflectivities  $s_j$ , temperatures  $T_j$  ( $j = 1, \dots, n$ ), ground temperature  $T_0$  and the sky brightness temperature  $T_{sky}$  (11).

### ***pfadc***

calculates the effective path length  $d'$  in a layer (33), using the effective propagation angle (59) and the total transmissivity (60).

### ***pfadi***

calculates the effective path length  $d'$  (33) in a layer of propagation angle  $\theta$  according to Snellius.

### ***polder***

is a subroutine to solve the *Polder and van Santen* [1946] Equation for spheroids  $A_1 = A_2 = 0.5 (1 - A_3)$ .

### ***polmix***

calculates the polarization mixing of the interface reflectivities of each layer (62), (63).

### ***rt***

computes the layer reflectivity  $r$  and transmissivity  $t$  from the two-flux coefficients  $\gamma_a'$ ,  $\gamma_b'$  and the path length  $d'$  (36), (37) and (38).

### ***sccoeff***

computes the six-flux scattering coefficients from snow structure information with different choices, expressed by the parameter *sccho*:

Equation (78) for *sccho*=8,

Equation (79) for *sccho*=10,

Equation (80) for *sccho*=11,

or the improved Born Approximation of Mätzler and Wiesmann (1999) for *sccho*=12.

Furthermore, transforms the coefficient to the two-flux scattering coefficient  $\gamma_b'$  (30).

Transforms the six-flux absorption coefficient  $\gamma_a$  to the two-flux absorption coefficient  $\gamma_a'$  (29).

```
function [gbih,gbiv,gs6,ga2i] = sccoeff(roi,Ti,pci,freq,epsi,gai,sccho,kq)
% calculates the scattering coefficient from structural parameters
% different algorithms can be chosen, by changing "sccho"
%     gbih: 2-flux scattering coefficient at h pol
%     gbiv: 2-flux scattering coefficient at v pol
%     gs6: 6-flux scattering coefficient
%     ga2i: 2-flux absorption coefficient
%     roi: density
%     Ti: physical temperature
%     pci: correlation length
%     freq: frequency
%     epsi: real part of relative dielectric constant of dry snow
%     gai: absorption coefficient
%     sccho: scattering coefficient algorithm chosen
%     kq: squared field ratio  $K^2$  (for sccho=12)
```

```

% Version history:
% 1.0b    wi 15.7.95
% 1.0     wi 23.9.97 bug fixed
% 1.1     wi 26.9.97 latest fit on experimental data was added (option 7)
% 1.2     wi 13.10.97 option 8 added, adapted scattering of a shell/sphere
% 1.3     wi 4.11.97 option 9, 10 and 11 added
% 1.4     wi 27.05.98 born approximation added (borna.m)
% 3.0     ma 03.04.2007 adapted to Version 3
% Uses:
% borna, epsicereal (both for sccho = 12 only)
% Copyright (c) 2007 by the Institute of Applied Physics,
% University of Bern, Switzerland

```

### *slred*

Given a special snow profile, then at each frequency  $f$  and incidence angle  $\theta_n$ , the following tasks have to be performed:

- Check if there is a volume scattering layer at all ( $2p_j > 4.7$ ). If there is no such layer, the snowpack emission model cannot be applied to this situation.
- Remove thin layers from the bottom until a scattering layer is found. The thickness of the scattering layer increases by the extent of the removed layers.
- Locate thin layers elsewhere from the table of the snow profile.
- Locate the thickest layer if more than one subsequent layer is found to be thin and ignore the others.
- Repeat until all thin layers have been identified.
- Compute the coherent reflectivities (at h and v polarization) of the thin layers and replace the interface reflectivities of the adjacent layers by the coherent reflectivities (54).
- Ignore volume scattering within a thin layer, e.g. remove it from the input table of scattering layers. Only regular layers are left. The new input table is now ready to be used by MEMLS.

### *vk2eps*

```

function result = vk2eps(roi,graintype)
% Computes volume fraction, K^2 (the squared ratio between internal
% and external E-field) and real diel. constant in the
% Effective-Medium Approximation (Polder and van Santen, 1946) of
% dry snow with given depolarization factors, A=A1=A2 and A3=1-2A
% all versus snow density, roi (graintype=1), for spheres
% (gaintype=2), or spherical shells (graintype=3).
% kq: squared E field ratio
% roi: dry snow density (g/cm3)
% graintype: 1 (snow), 2 (spheres), 3 (thin sph. shells)
% Version history:
% 1.0     wi 29.5.98,
% 3.0     lb 2.3.2007, cm 2.4.2007
% Uses: epsr
% Copyright (c) 2007 by the Institute of Applied Physics,
% University of Bern, Switzerland
result=[v, kq, epseff];

```

## 5. Examples

In these examples (80) was used to determine the six-flux scattering coefficient  $\gamma_s$ .

### 5.1 Emissivity of a snowpack

Table 1 shows the snow profile that was used. It is a winter snow situation of Weissfluhjoch Davos, Switzerland. The snow height is 60.3 cm. The top layer is a new snow layer, above a thin crust. At the bottom coarse-grained snow is observed.

**Table 1:** Snow profile. Data is taken from Wiesmann et al. [1996]. Symbols are defined as follows:  $T_{\text{snow}}$ , physical snow temperature;  $W$ , liquid water content;  $\rho$ , density;  $d$ : thickness of the layer;  $p_{\text{ec}}$ : exponential correlation length. The layer number increases from bottom to top.

Date/ layer No.	$T_{\text{snow}}$ [K]	$W$ [%]	$\rho$ [kg/m <sup>3</sup> ]	$d$ [cm]	$p_{\text{ec}}$ [mm]
21.12.95					
1	273.0	0.00	259.0	25.0	0.1702
2	272.0	0.00	177.0	15.0	0.0961
3	266.5	0.00	400.0	0.3	0.0000
4	271.4	0.00	109.0	20.0	0.0701

The resulting snow emissivity is shown in Figure 6. The lines indicate computed data while the symbols indicate measurements. Note the increase of polarization difference for frequencies below 35 GHz. Below 35 GHz layer No. 3 is considered as a coherent scatterer. The behavior of this layer leads to a good agreement between the measured and computed emissivity. The parameters of layer No. 3 could not be measured in-situ. They had to be defined by experience. However this example shows the importance of the exact treatment of thin layers.

The increase of the in-situ data at small incidence angles is due to a shadowing effect by the radiometer system.

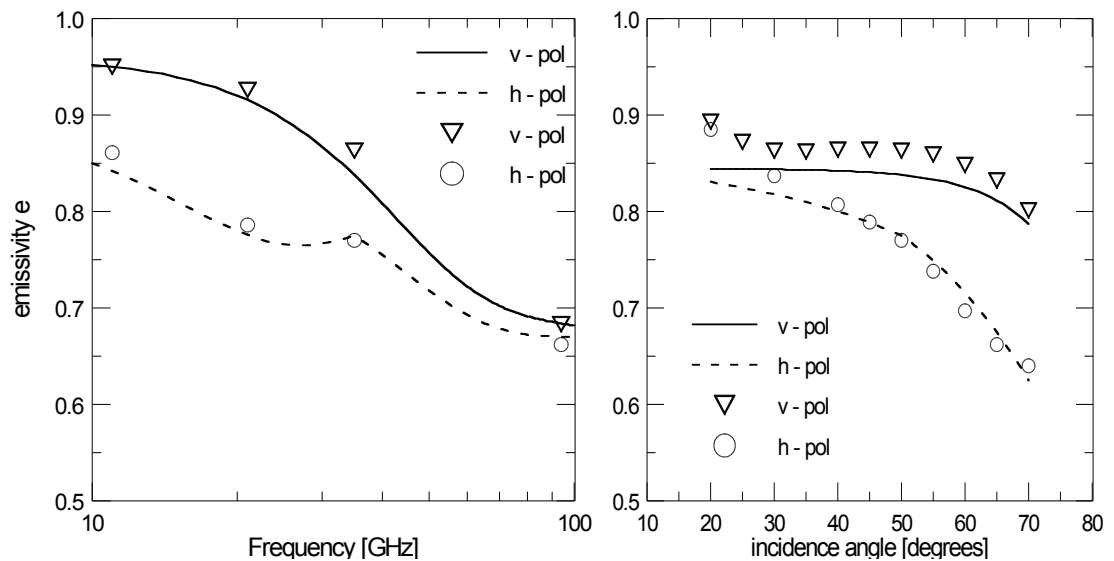


**Figure 6:** Left: Emissivity versus frequency of the modified winter snow pack on 21 Dec. 1995. Right: Emissivity versus incidence angle of the same snow pack.

Table 2 shows the intermediate values of the simulation. The h and v indices stand for the horizontal and vertical polarization, respectively. Layer 3 disappeared because it is a thin layer at 30 GHz.

**Table 2:** Intermediate data of the example simulation at 30 GHz and 50° incidence angle.

$j$	$\theta$ [°]	$d'$ [cm] l	$s_h$	$s_v$	$r_h$	$t_h$	$r_v$	$t_v$	$D_h$ [K]	$D_v$ [K]
0	39.4		0.0828	0.0472						
1	45.4	26.0	0.0096	0.0004	0.0879	0.8064	0.0879	0.8064	239.6	242.1
2	46.7	14.2	0.1065	0.0039	0.0141	0.9668	0.0141	0.9668	235.3	239.2
4	50.0	14.5	0.0034	0.0000	0.0097	0.9778	0.0097	0.9778	209.6	236.3
Air									208.8	236.3

## 5.2 Simulation of spatial snowpack emissivity variations

In *Sturm and Holgren* [1994] a snow profile of a cross section at Imnavit Creek, Alaska, for November 18<sup>th</sup>, 1989, is given. The snow is characterized by snow type, layer thickness and soil temperature. The corresponding layer temperatures were interpolated from the soil and air temperatures. The correlation lengths and densities were specified using typical values from our snow sample catalog (*Wiesmann*, [1998]). The spatial variation of the emissivity at 35 GHz (considering an incidence angle of 50°) and the snow height is shown in Figure 7. As expected an anticorrelation between these two parameters can be observed. Due to the strong scattering of the depth hoar layers the emissivities are below 0.7. At a displacement of 2m the depth hoar layers are very thin leading to an increase of the emissivity up to 0.9. This example shows the strong spatial variation of the emissivity of tundra snow situations. To compare the computed data with satellite or land-based sensors the extent of the footprint has to be taken into account.

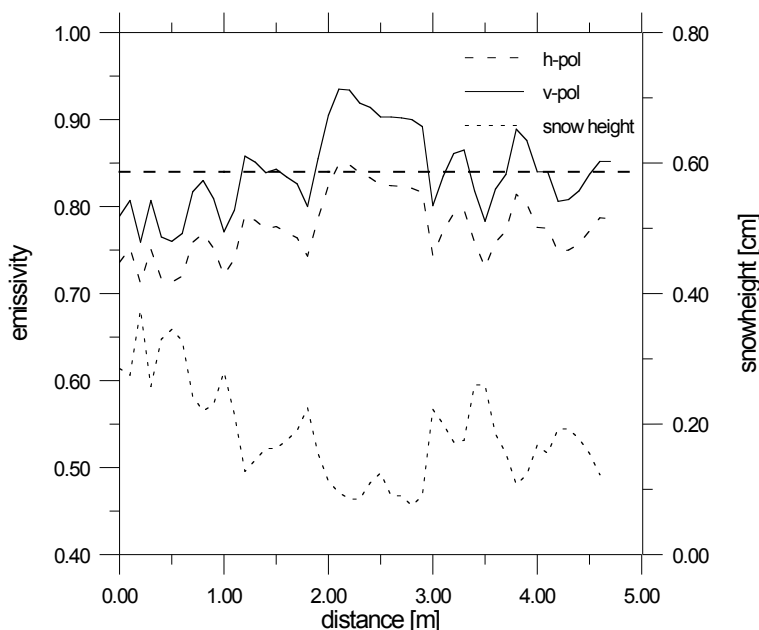


**Figure 7:** Emissivity (upper lines) and snowheight (lower line) versus distance. Observation frequency is 37 GHz and incidence angle is 50°. Input data is taken from *Sturm and Holmgren* [1994]. The horizontal line indicates the apparent emissivity obtained within the nearest SSM/I sample at 37 GHz, v-pol.

## 6. References

- Colbeck, S., E. Akitaya, R. Armstrong, H. Gubler, J. Lafeuille, K. Lied, D. Mc Clung, and E. Morris, *The international classification for seasonal snow on the ground*, Int. Comm. on Snow and Ice of the Int. Assoc. of Sci. Hydrol. and Int. Glaciol. Soc. (1990). Available from CIRES, Box 449, Univ. of Colo., Boulder, CO 80309. See also new version (2009)
- Ellison, W. "Permittivity of pure water at standard atmospheric pressure, over the frequency range 0 – 25 THz and the temperature range 0 – 100 C", J. Chem. Ref. Data, Vol. 36 (1), 1-18 (2007).
- Hallikainen M., F. Ulaby, M. Abdelrazik: "Dielectric properties of snow in the 3 to 37 GHz range", IEEE Trans. On Antennas and Propagation, Vol. AP-34, No. 11, pp. 1329 - 1340, 1986.
- Ishimaru A., *Wave propagation and scattering in random media*, Vols. 1 and 2, Academic Press, Orlando (1978).
- Liebe H.J., G.A. Hufford, and T. Manabe, "A Model for the complex permittivity of water at frequencies below 1 GHz", Internat. J. IR and mm waves, Vol. 12, No. 7, 659-675 (1991).
- Looyenga H., "Dielectric constant of heterogeneous mixtures", Physica, Vol. 21, pp. 401 - 406 (1965).
- MathWorks The, Inc., "Matlab, the language of technical computing", 24 Prime Park Way, Natick, MA 01760-1500 (1996).
- Mätzler C., H. Aebischer, E. Schanda: "Microwave dielectric properties of surface snow", IEEE J. Oceanic Eng., Vol. OE-0, pp. 366 - 371 (1984).
- Mätzler C., "Applications of the Interaction of Microwaves with the Seasonal Snow Cover", Remote Sensing Reviews, Vol. 2, pp. 259 - 387 (1987).
- Mätzler C.: "Microwave permittivity of dry snow", IEEE Transactions on Geosc. And Rem. Sens., Vol. 34, No. 2, pp. 573 - 581 (1996a).
- Mätzler C., "Notes on microwave radiation from snow samples and from a layered snowpack", IAP Research Report 96-9, University of Bern, Switzerland, (1996b), updated (2004).
- Mätzler C., and A. Wiesmann, "Effective propagation angle and polarization mixing in a snowpack", IAP Research Report 97-11 University of Bern, Switzerland, 1997.



- Mätzler C., "Improved Born Approximation for scattering of radiation in a granular medium", *J. Appl. Phys.*, Vol. 83, No. 11, pp. 6111-6117 (1998a).
- Mätzler C., "Microwave properties of ice and snow", in B. Schmitt et al. (eds), *Solar System Ices*, pp. 241 - 257 (1998b).
- Mätzler C. and A. Wiesmann, "Extension of the Microwave Emission Model of Layered Snowpacks to Coarse-Grained Snow", *Remote Sensing of Environment*, Vol. 70, No. 3, pp. 317-325 (1999).
- Mätzler C. (Ed.), P.W. Rosenkranz, A. Battaglia and J.P. Wigneron (Co-Eds.), *Thermal Microwave Radiation - Applications for Remote Sensing*, IET Electromagnetic Waves Series 52, London, UK (2006).
- Mishima O., D. Klug, and E. Whalley, "The far-infrared spectrum of ice in the range 8 - 25 cm<sup>-1</sup>: Sound waves and difference bands, with application to Saturn's rings", *J. Chem. Phys.*, 78, 6399 - 6404 (1983).
- Polder D., and J.H. van Santen, "The effective permeability of mixtures of solids", *Physica*, Vol. 12, (5), pp. 257 - 271 (1946).
- Pulliainen J., K. Tigerstedt, W. Huining, M. Hallikainen, C. Mätzler, A. Wiesmann, and C. Wegmüller, *Retrieval of geophysical parameters with integrated modeling of land surfaces and atmosphere (models/inversion algorithms)*, final report, Eur. Space Agency/Eur. Space Res. and Technol. Cent., Noordwijk, Netherlands (1998).
- Reber B., C. Mätzler, E. Schanda, "Microwave Signatures of Snow Crusts: Modelling and Measurements", *International Journal of Remote Sensing*, Vol. 8, pp. 1649 - 1665 (1987).
- Sturm M., and J. Holmgren, "Effects of microtopography on texture, temperature and heat flow in Arctic and sub-Arctic snow", *Annals of Glaciological Society*, Vol. 19, pp. 63 - 68 (1994).
- Tiuri, M.E., A. Sihvola, E. Nyfors, and M. Hallikainen, "The complex dielectric constant of snow at microwave frequencies", *IEEE J. Oceanic Eng.*, OE-9, 377 - 382 (1984).
- Ulaby F., R. Moore, A. Fung, *Microwave Remote Sensing Active and Passive, Vol. III*, Artech House, pp. 2022 - 2025 (1986).
- Weise T., "Radiometric and Structural Measurements of Snow", Ph.D. thesis, Institute of Applied Physics, University of Bern, Switzerland (1996).

- Wiesmann A., T. Strozzi, and T. Weise, "Passive Microwave Signature Catalogue of Snowcovers at 11, 21, 35, 48 and 94 GHz", IAP Research Report 96-8 University of Bern, Switzerland (1996).
- Wiesmann A., "Catalog of Radiometric and Structural snow sample measurements", IAP Research Report 97-1, University of Bern, Switzerland (1997).
- Wiesmann A. and C. Mätzler, "Coherent scattering effects in a snowpack", IAP Research Report No. 97-7, Microwave Department, Institute of Applied Physics, University of Bern (1997).
- Wiesmann A., C. Mätzler and T. Weise, "Radiometric and structural measurements of snow samples", Radio Sci. Vol. 33 , No. 2 , p. 273-289 (1998)
- Wiesmann A., and C. Mätzler, "Microwave emission model of layered snowpacks", Remote Sensing of Environment, Vol. 70, No. 3, pp. 307-316 (1999).